ANALYSIS AND CONTROL RESEARCH ON INTAKE NOISE ISSUES OF HEAVY-DUTY COMMERCIAL VEHICLE AIR COMPRESSORS

Wang Shaocun[1], Wang Xinlong[1], Ning Tingzhou[1], Bi Yuqiang[1]*
[1]Department of Intelligent Manufacturing, Jinan Vocational College, Jinan 250103, China
E-mail: jnzyxyntz@jn.shandong.cn

Abstract - Controlling intake noise has always been a challenge in the commercial vehicle industry. In the field of heavy-duty commercial vehicles, due to the strong excitation energy and broad noise frequency band of air compressors, accurately diagnosing noise characteristics and effectively controlling these issues have become common challenges in the industry. This paper addresses the noise issue of a specific model of heavy-duty commercial vehicle's air compressor. Based on the key frequencies and distribution characteristics, a targeted control scheme was developed. After on-site validation, the control scheme demonstrated ideal performance, effectively mitigating the air compressor noise issue, providing a valuable reference for controlling air compressor noise in heavy-duty commercial vehicles.

Keywords: Heavy-duty commercial vehicle, Air compressor, Noise control, Noise spectrum, Simulation and experiment.

1. Introduction

With the increasing youthfulness of drivers and passengers and the improvement of social living standards, market demands for both interior and exterior noise levels in commercial vehicles have significantly risen [1-4]. As a key component of commercial vehicles, the air compressor plays a crucial role in supplying high-pressure air for the braking system, but it is also a major noise source. It exhibits significant noise impacts under common operating conditions, necessitating targeted control measures. However, due to the strong excitation energy and wide noise frequency range of air compressors, efficiently and cost-effectively implementing noise control improvements has become a challenging issue in the commercial vehicle industry [5-8].

To effectively control the noise issue of air compressors in heavy-duty commercial vehicles, this paper started by identifying the key characteristics of the system based on the manifestations of the noise problem. It then proposed a control solution and conducted simulation analysis. To verify the effectiveness of the proposed solution, a real vehicle test was conducted using the solution prototype. The verification results indicated that the control solution could perform well and effectively mitigate the noise issue of air compressors in heavy-duty commercial vehicles [9-12].

2. Problem Manifestation

2.1 Introduction to the Test Setup

Figure 1 shows the test setup diagram for the ear-side noise testing of a particular model of commercial vehicle, where Figure 1(a) depicts the original state without a muffler and Figure 1(b) shows the improved state with a muffler installed.

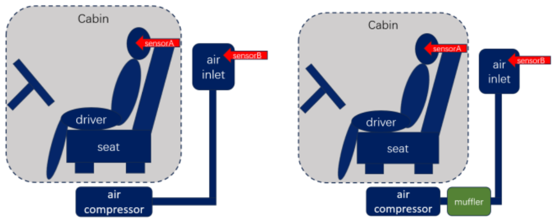

(a) Without muffler (b) With muffler

Figure 1: Test setup diagram

The positions of the sensors in both test states are identical, with sensor A located next to the driver’s ear, facing forward to measure interior noise, and sensor B positioned beside the air inlet, also facing forward, to capture exterior noise. Additionally, the compressor is located beneath the cabin, while the air inlet is positioned behind the cabin, connected to the compressor via a conduit. The compressor is powered by the engine. For test parameters, the sensors have a bandwidth of 10 kHz and a resolution of 0.25 Hz. The muffler in the improved setup is installed in the connecting duct between the compressor and the air inlet, as shown in Figure 1(b) [13-14].

2.2 Interior Noise Analysis

An idle test was conducted on the test vehicle under stationary conditions, with the engine running at 500 rpm, and the primary vibration frequency was 25 Hz. One of the windows is closed when the compressor is not working, meaning that the compressor is in a condition of unloaded idle running. When the compressor is working, the other window is opened, meaning that the compressor is in a condition of outputting load. The original state testing of the noise at the ear (sensor A), the test time is 10s, and the time-domain signal of the noise at the ear is obtained.

Figure 2 and Figure 3 respectively show the noise spectrum near the driver's ear when the air compressor is off and on, with the horizontal axis representing frequency and the vertical axis representing sound pressure amplitude.

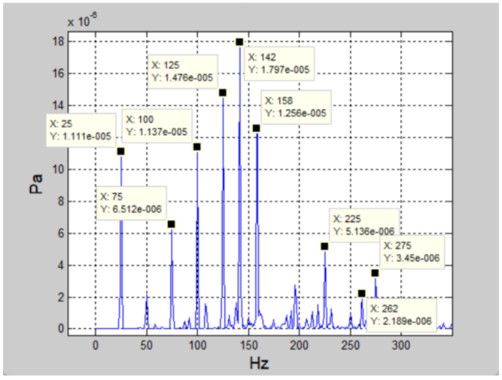

Figure 2: The noise spectrum near the driver's ear when the air compressor is off

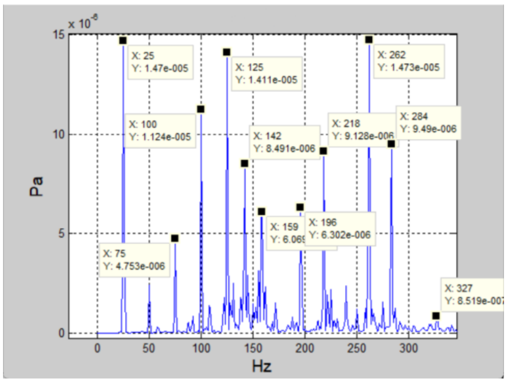

Figure 3: The noise spectrum near the driver's ear when the air compressor is on

Comparative analysis of the noise spectra under the two states shows that when the air compressor is off, the energy of the interior noise near the driver's ear is mainly distributed between 0-400 Hz, with the primary energy at the engine's main vibration frequency and its harmonic orders. Additionally, there are two significant singular peaks at 142 Hz and 158 Hz. When the air compressor is on, the energy of the interior noise near the driver's ear is still mainly distributed between 0-400 Hz, with the primary energy at the engine's main vibration frequency and its harmonic orders. However, there are additional significant peaks at 142 Hz, 159 Hz, 196 Hz, 218 Hz, 262 Hz, and 284 Hz. Compared to when the air compressor is off, the 262 Hz peak energy is particularly prominent when the compressor is on, and the 218 Hz and 284 Hz peaks are also significant.

2.3 Exterior Noise Analysis

With the same conditions and test synchronisation as the interior noise test, the original state test of the exterior noise (sensor B) was conducted for 10s to obtain the time-domain signal of the exterior noise.

Figure 4 and Figure 5 respectively show the noise spectrum at the exterior noise measurement point when the air compressor is off and on, with the horizontal axis representing frequency and the vertical axis representing sound pressure amplitude.

Comparative analysis of the noise spectra under the two states shows that when the air compressor is off, the energy of the exterior noise is mainly distributed between 0-2 kHz, with the energy between 600 Hz and 900 Hz being particularly prominent. The frequency range corresponds to the 0-400 Hz range for the interior noise, with the primary energy at the engine's main vibration frequency and its harmonic orders. The 142 Hz peak is also present. When the air compressor is on, in the 0-400 Hz range, the interior noise near the driver's ear is mainly driven by the engine's primary vibration frequency and its harmonic orders. Significant peaks are observed at 240 Hz, 262 Hz, and 284 Hz. Compared to when the air compressor is off, the 262 Hz peak energy is particularly prominent, and there is noticeable energy between 218 Hz and 305 Hz, with the 240 Hz to 284 Hz range being especially prominent.

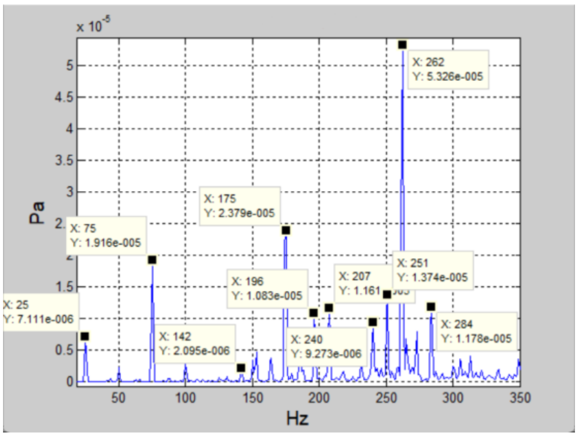

Figure 4: The noise spectrum outside the vehicle when the air compressor is off

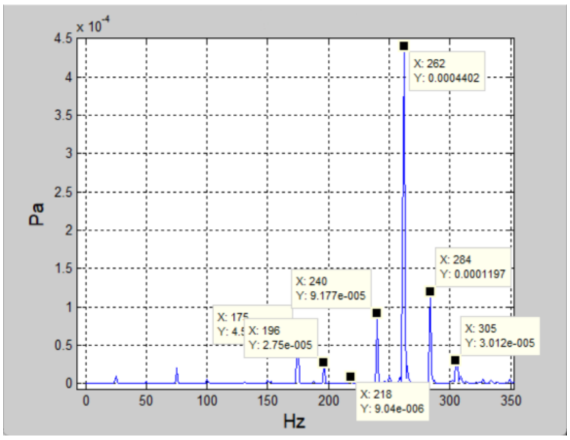

Figure 5: The noise spectrum outside the vehicle when the air compressor is on

In summary, the noise corresponding to the air compressor has a centre frequency of 262 Hz, with noticeable energy in the 240 Hz to 284 Hz range.

3. Mechanism Analysis and Improvement Simulation

To identify the overall vibration and noise mechanism issues, it is necessary to combine the subjective evaluation results. The subjective evaluation results (5 points, fail) show that during the operation of the air compressor, there is a significant "thumping" noise inside and outside the vehicle, and the vibration felt inside the vehicle intensifies. This also indicates that the excitation vibration energy level of the air compressor during operation is high, and the noise impact is significant.

The air compressor noise problem is identified as a resonant cavity noise issue, similar to the noise performance of an engine piston cylinder. However, the piston cylinder noise is effectively muffled on the intake side using an air filter. The absence of a muffler on the intake side of the air compressor is the direct cause of the air compressor noise, and the noise further radiates outward through the intake duct, resulting in more widespread pulsating noise issues.

The solutions to the air compressor intake noise problem mainly include three approaches: expansion chamber, Helmholtz resonator, and quarter-wave tube. Based on the selectivity and stringency for noise, the three approaches are ranked as follows: expansion chamber < Helmholtz resonator < quarter-wave tube. Although the expansion chamber is less effective in maximum noise attenuation, it is widely used due to its broad frequency selectivity and low cost. However, its size requires comprehensive consideration during practical application. Considering noise attenuation performance and cost, the expansion chamber is chosen as the improvement solution.

4. Control Scheme Simulation Analysis

The schematic diagram of the improvement solutions is shown in Figure 6. In the diagram, scheme a represents the expansion chamber solution without an internal perforated pipe structure, while scheme b represents the expansion chamber with an internal perforated pipe.

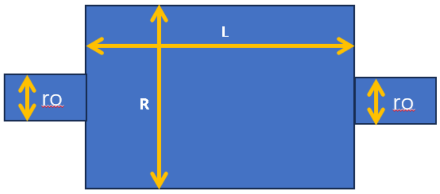

(a) The expansion chamber solution without an internal perforated pipe structure

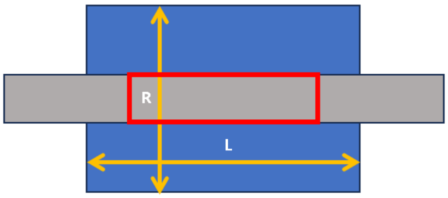

(b) The expansion chamber with an internal perforated pipe

Figure 6: Schematic diagram of improvement solutions

Notes: R represents the diameter of the expansion cavity, L represents the length of the expansion cavity, and the red box area represents the perforation area.

A finite element simulation model of the muffler is established to simulate and analyse the muffling performance of the improved scheme in the problem frequency domain [15-17]. The simulation results of the noise attenuation performance of the expansion chamber are shown in Figure 7. The dashed line represents the solution with an expansion chamber length of 200 mm, while the solid line represents the solution with an expansion chamber length of 324 mm. Each condition simulates five different internal diameters of the expansion chamber: 90 mm, 100 mm, 110 mm, 120 mm, and 150 mm. Comparative analysis shows that for the solution with an expansion chamber length of 324 mm, as the internal diameter increases, the noise attenuation performance improves. When the internal diameter reaches 120 mm, the solution achieves a 20 dB noise attenuation capability in the 200-300 Hz range. Solutions with an internal diameter smaller than 120 mm do not achieve this performance. For the solution with an expansion chamber length of 200 mm, as the internal diameter increases, the noise attenuation performance also improves. When the internal diameter reaches 140 mm, the solution achieves a 20 dB noise attenuation capability in the 205-300 Hz range.

Solutions with an internal diameter smaller than 140 mm do not achieve this performance.

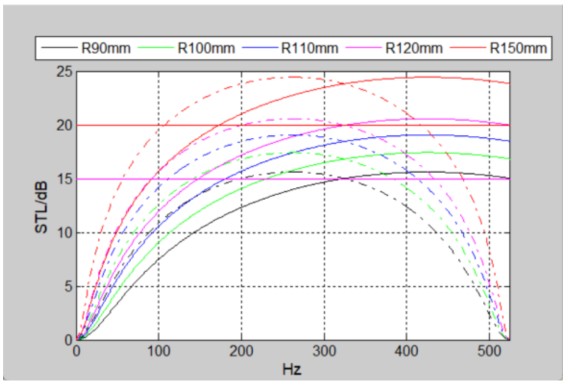

Figure 7: Noise attenuation performance (Solid line: L=200mm, Dashed line: L=324mm)

Based on the analysis above, the design parameters for the expansion chamber verification samples are as follows:

- The intake and exhaust ports have the same length, internal diameter, and external diameter parameters, which are 50 mm, 26 mm, and 30 mm, respectively.
- Sample 1: Expansion chamber, internal diameter R = 120 mm, internal length L = 324 mm.
- Sample 2: Expansion chamber, internal diameter R = 140 mm, internal length L = 200 mm.

A finite element simulation model of the muffler is established to simulate and analyse the muffling performance of the improved scheme in the problem frequency domain. The simulation results of the noise attenuation performance of the expansion chamber with an internal perforated pipe are shown in Figure 8 and Figure 9. Figure 8 shows the analysis results for the scheme with a 6 mm perforation diameter, while Figure 9 shows the analysis results for the scheme with a 5 mm perforation diameter. Comparative analysis shows that for the scheme with an expansion chamber + internal perforated pipe (6 mm perforation diameter), the 15 dB noise attenuation capability corresponds to frequency bands of 193 Hz and 375 Hz, while the 20 dB capability corresponds to frequency bands of 221 Hz and 324 Hz. These frequency bands generally cover the primary frequency range of the air compressor noise issue, and the centre frequency aligns with the air compressor noise problem's centre frequency. For the scheme with an expansion chamber + internal perforated pipe (5 mm perforation diameter), the 15 dB noise attenuation capability corresponds to frequency bands of 182 Hz and 343 Hz, while the 20 dB capability corresponds to frequency bands of 209 Hz and 299 Hz. These bands also cover the primary frequency range of the air compressor noise issue. Although there is a deviation from the centre frequency of 262 Hz, the noise attenuation capability at 262 Hz still reaches 20 dB.

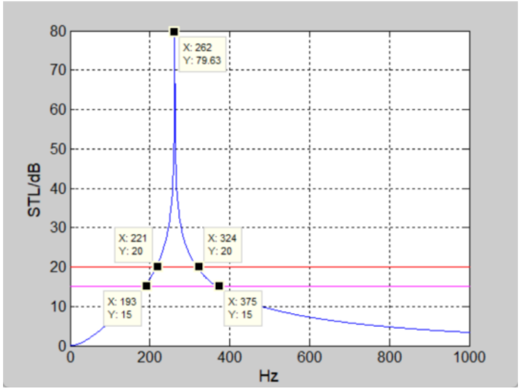

Figure 8: Noise attenuation performance (6 mm perforation diameter)

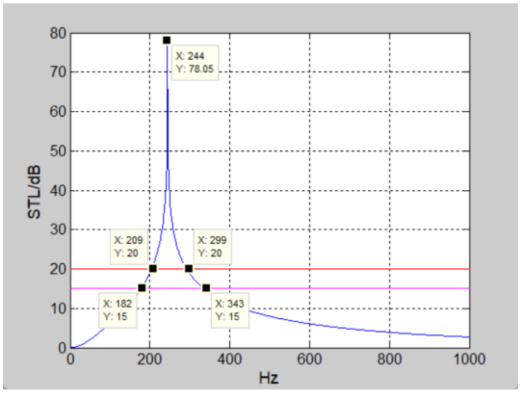

Figure 9: Noise attenuation performance (5 mm perforation diameter)

- Sample 3: Expansion chamber + internal perforated pipe, 6 mm perforation diameter, 16 perforations (4 in each row, with a 90-degree circumferential spacing, 4 rows in total), approximately 30 mm spacing.
- Sample 4: Expansion chamber + internal perforated pipe, 5 mm perforation diameter, 20 perforations (5 in each row, with a 90-degree circumferential spacing, 4 rows in total), approximately 25 mm spacing.

5. Verification Analysis

Samples 1 (the first group) and 3 (the second group) were used as verification measures and applied to the test vehicle for real vehicle validation studies. The primary test conditions were the overall noise at idle and the spectral performance at idle, with the verification state divided into subjective evaluation and objective evaluation.

Objective Evaluation:

First, the overall noise analysis is shown in Figure 10. The noise test results for the original state, first group solution, and second group solution under idle conditions are presented in the figure. The results show that compared to the original state, both the first group solution and the second group solution significantly improve noise levels. Under the air charging state, the second group showed the most significant improvement, reducing the interior noise to within 52 dB(A), achieving an ideal noise attenuation effect. In the non-air charging state, the second group solution also demonstrated the most significant improvement compared to the original state, reducing the interior noise to within 52 dB(A), achieving comprehensive noise attenuation.

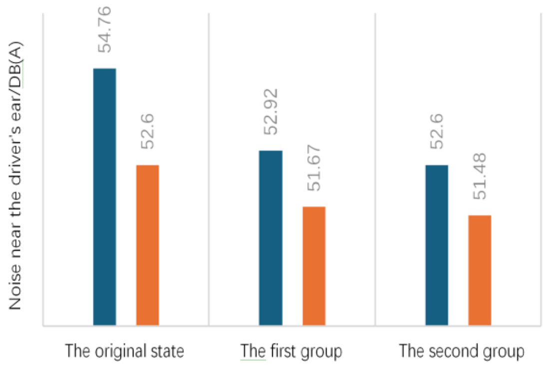

Figure 10: Overall noise verification results

Notes: ■ represents the air charging state, ■ represents the non-air charging state.

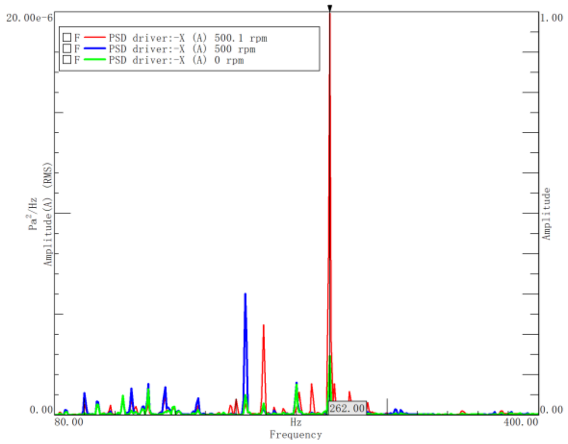

Figure 11: Noise spectrum verification results

Notes: Red represents the original state, dark blue represents the first group, and light green represents the second group.

In terms of objective evaluation, the spectral performance analysis continues as shown in Figure 11. The noise test results for the original state, first group solution, and second group solution under air charging idle conditions are shown in the figure. The results demonstrate that compared to the original state, both the first and second group solutions exhibit significant noise attenuation in both the centre frequency and the side frequency bands. The second group solution showed the most significant improvement compared to the original state, achieving sufficient noise attenuation.

Subjective Evaluation:

The subjective evaluation also identified the overall vibration and noise performance. Compared to the original state's subjective evaluation result (5 points, fail), where there was significant "thumping" noise both inside and outside the vehicle during the air compressor operation and an increased sense of vibration inside the vehicle, the improved state's subjective evaluation result was 7.5 points, with no obvious "thumping" noise inside or outside the vehicle, and the sense of vibration inside the vehicle was significantly reduced. The subjective evaluation results were consistent with the objective evaluation.

The above conclusions validate the relevance, rationality, and effectiveness of the mechanism analysis, improvement solution, and the simulation results of the improvement solution.

6. Conclusions

The air compressor noise issue is identified as a resonant cavity noise problem, similar to the noise performance of an engine piston cylinder. The absence of a muffler on the intake side is the direct cause of the air compressor noise, which further radiates outward through the intake duct, causing more widespread pulsating noise issues.

The improvement solution proposed in the paper, as demonstrated by simulations, achieves a 20 dB noise attenuation capability in the 200-300 Hz range, covering the main frequency range of the air compressor noise issue, and the centre frequency aligns with the air compressor noise problem's centre frequency.

The validation of the improvement solution shows that it has reduced the interior noise to within 52 dB(A), achieving an ideal noise attenuation effect. The noise attenuation was significant for both the centre frequency and the side frequency bands, achieving sufficient noise attenuation, and the subjective evaluation improved by 2.5 points. These results validate the relevance, rationality, and effectiveness of the mechanism analysis, improvement solution, and the simulation results.

Acknowledgements

This work was supported by 2023 Jinan Vocational College Research Project: XHS2425A×50 High-Speed Fixed Beam Gantry Boring and Milling Machining Centre (KYJB202307).

References

[1] Li Yijiang, Chen Ke. Vehicle's Internal Noise Source Identification Based on CEEMDAN-WSVD Combined Crosstalk Cancellation Method[J]. Noise and Vibration Control,2024,44(4):224-230.
[2] Zhou Hao, Feng Qingsong, Yin Huatuo, Luo Xinwei, Liu Qingjie. Analysis of Noise Characteristics and Contribution Rate in Urban Rail Transit Vehicles[J]. Noise and Vibration Control,2023,43(6):157-162+172.
[3] Li Yi, Xie Yunhe, He Jiayang. Identification of sources of noise emitted by accelerating vehicle

based on transfer path and its improvement[J]. Internal Combustion Engine & Powerplant,2024,41(2):48-52.
[4] Wang Chaoliang, Wu Xiaolong, Zhang Liangtao, Zhang Chao, Luo Yunke, Song Lizong. Exterior Noise Source Identification Test of Trains on Suburban Elevated Rail Transit Bridges[J]. Noise and Vibration Control,2023,43(2):185-189+236.
[5] Wang Hu, Yu Jinning, Zhao Sheng, Liu Jinqiu. Study on Noise Hazard Analysis and Control Technology of Large Air Compressor in a Thermal Power Plant[J]. Safety Health & Environment,2022,22(5):11-14.
[6] Li Jinlu, Geng Maofei, Jiang Huijun, Wang Le, Cui Dong, Li Xiaosa. Aerodynamic noise optimization design of dry twin screw air compressor[J]. Hydraulics Pneumatics & Seals,2023,43(4):7-10.
[7] Shen Yaorui, Bao Huanhuan, Liu Qi, Fu Jianqin. Design and Noise Reduction Analysis of a Resistant Muffler for Fuel Cell Centrifugal Air Compressors[J]. Chinese Journal of Automotive Engineering,2024,14(4):706-714.
[8] Wang Demeng, Yin Hongbin, Zhang Jun, Yu Xin long, Zhang Xueyi. Optimization design of permanent magnet motor for vibration reduction fuel cell air compressor[J]. Small & Special Electrical Machines,2023,51(10):19-23.
[9] Li Dong, Wang Qi, Yang Shanju, Zhang Lijun, Zhu Yiming, Zhu Xuewei. Experimental and Simulation Study on Performance of Air-suspending Centrifugal Air Compressor for Hydrogen Cell[J]. Chinese Journal of Turbomachinery,2024,66(3):29-34.
[10] Lei Jun, Zhang Wenfu, Wang Qin, Yuan Shaofei, Wu Anqi, Wang Jin, Zhang Jian. Design and testing of a continuous automatic forming device for bamboo spoons[J]. Journal of Forestry Engineering,2023,8(5):152-159.
[11] Chen Guo, Wang Chang, Wu Jing, Zhang Enhao, Wu Di. Mechanical performance of nailed connections between laminated bamboo lumber and oriented strand board[J]. Journal of Forestry Engineering,2023,8(2):75-81.
[12] Bai Jie, Wen Wei, Zhou Hua, Ding Junhao. Bearing capacity of the connection between phosphogypsum panels and wood structure walls with bone column nails[J]. Journal of Forestry Engineering,2023,8(1):165-171.
[13] He Xuyang, He Yayin, Zhang Wei, Wang Kai. Design and performance analysis of muffler for twin-screw air compressor[J]. Science Technology and Engineering,2024,24(8):3222-3228.
[14] Shen Rui. Noise analysis and muffler optimization design of air intake system of a heavy truck engine air compressor [D]. Zhejiang University,2024.
[15] Li Guojun, Cai Yaoyu, Chen Shuming, Zhao Yongnan, Qin Duo. Simulation and Analysis of Induction Noise in Commercial Vehicles Coupled with Air Compressor[J]. Automobile Technology, 2024, (9):32-37.
[16] Shen Yi, Yang Zhengyin, Sun Xiaoqing, Yuan Qingze, Liang Huafang, Hu Wei. Analysis and Optimization of Aerodynamic Noise Characteristics of Double-stage ElectricAir Compressors[J]. Noise and Vibration Control,2024,44(5):82-87+132.
[17] Zhao Tian, Yu Lei, Fan Lingju, Liu Zhiguo, Song Hongguang,Jiang Ling. Design and Test Research of the Rubber Damper of Air Compressor for a Metro Car[J]. Rolling Stock,2023,61(6):59-65.